



Research Project co-funded by the
European Commission
Research Directorate-General
6th Framework Programme
FP6-2002-Space-1-GMES
Ocean and Marine Applications
Contract No. AIP3-CT-2003-502885



MERSEA IP

Marine EnviRonment and Security for
the European Area - Integrated Project

Ice drift monitoring from low resolving sensors: an alternative method and its validation against in-situ data.

Ref: [MERSEA_WP02_METNO_STR_005_1B_pre]
2008-10-13

AUTHORS:

Thomas Lavergne, S. Eastwood, H. Schyberg and L. A. Breivik



Co-ordinator:

Institut Français de Recherche pour l'Exploitation de la Mer - France

Table of Content

1. INTRODUCTION.....	4
2. VALIDATION OF ICE DRIFT PRODUCT AGAINST IN-SITU DRIFTERS TRAJECTORIES.....	5
2.1. PRESENTATION OF THE DATASETS.....	5
2.1.1. <i>Low resolution ice drift estimates from pair of satellite images.....</i>	<i>5</i>
2.1.2. <i>In situ estimates of sea-ice drift.....</i>	<i>7</i>
2.2. VALIDATION RESULTS.....	8
2.3. CONCLUSIONS AND FURTHER RESEARCH.....	9
3. MERGING ICE DRIFT DATASETS FROM DIFFERENT SOURCES.....	10
3.1. JUSTIFICATION FOR THE MERGING AND CURRENTLY IMPLEMENTED METHODS.....	10
3.2. ASSESSING THE UNCERTAINTY IN ICE DRIFT ESTIMATES ACQUIRED FROM PAIRS OF IMAGES.....	11
3.2.1. <i>Qualitative assessment.....</i>	<i>11</i>
3.2.2. <i>Quantitative assessment.....</i>	<i>13</i>
3.3. LIMITS TO MERGING ICE DRIFT DATASETS FROM DIFFERENT SENSORS.....	14
3.3.1. <i>Accounting for the exact time span of the ice drift products.....</i>	<i>14</i>
3.3.2. <i>Case study: 48h ice drift generated by a low pressure system traveling over the ice shelf north of Siberia. On the importance of the exact time period.....</i>	<i>16</i>
3.4. CONCLUSION ON MERGING OF ICE DRIFT DATASETS.....	17
4. ACKNOWLEDGEMENTS.....	18
5. REFERENCES.....	19

Document Change Record

Author	Modification	Issue	Date
Thomas Lavergne	First released version		06/06/2008

Acronyms:

AVHRR	Advanced Very High Resolution Radiometer
AMSR-E	Advanced Microwave Scanning Radiometer
EUMETSAT	European Organisation for the Exploitation of Meteorological Satellites
OSI SAF	Ocean and Sea Ice Satellite Application Facility
met.no	The Norwegian Meteorology Institute
MCC	Maximum Cross Correlation
CMCC	Continuous MCC
DMCC	Discrete MCC
PDF	Probability Distribution Function
SAR	Synthetic Aperture Radar
SSM/I	Special Sensor Microwave Imager
V-pol/H-pol	Vertical / Horizontal polarization

1. INTRODUCTION

A processing chain has been developed at met.no to estimate 48h sea-ice drift between pairs of daily averaged, low resolution images acquired by a variety of instruments. If successful, this research effort should provide the base for the EUMETSAT Ocean and Sea Ice Satellite Application Facility low resolution ice drift product.

The aim of this report is to present early validation results for this product against in-situ drifters in the Arctic, during winter 2007-2008. Results illustrate that ice displacement vectors retrieved with the new method compare better to ground truth than those obtained with the classic Maximum Cross Correlation technique.

In a second part, we present results of investigations on merging ice drift datasets produced from different sensors. Although the merging is only considered between products of similar spatial and temporal resolution, hints are given on how to achieve this merging optimally. We also present a case-study where the merging of two datasets would lead to degrading the quality of the retrieval unless some new strategy which takes into account the sensing start time is designed.

2. VALIDATION OF ICE DRIFT PRODUCT AGAINST IN-SITU DRIFTERS TRAJECTORIES

2.1. Presentation of the datasets

2.1.1. Low resolution ice drift estimates from pair of satellite images

Ice drift monitoring from satellite images necessitates at least two images of the same area, taken at different times. The drift (displacement) is then retrieved by some more or less elaborated image comparison techniques able to link an intensity feature from the first image to its “drifted” equivalent in the second.

Algorithms can be clustered into 3 main groups: block-based methods, optical flow differential methods and direct assimilation of the images in a geophysical model. Retrieval methods from the first category are the most widely used (see e.g. Maslanik et al. (1998)), and are applied successfully to high (SAR, AVHRR) and low (SSM/I, various scatterometers, AMSR-E) resolution sensors. While applying a variety of refinements, they usually boil down to finding, for each block (alternatively named sub-image, pattern, correlation window...) in the image, the best displacement vector (x,y) . The latter is defined as the vector (out of a poll of candidates) for which the chosen image comparison metric takes its best value. For ice drift, most frequently, the metric of choice is the Cross Correlation between a block in image 1 and a block in image 2 and the “best” operator is the maximum, hence the name for this method: Maximum Cross Correlation (MCC). The size of the poll of candidates is related to a maximum drift speed which, once integrated over the time span between the two images, defines an extent inside which all drift pairs (x_i,y_i) should be tested. This makes the MCC a truly discrete optimization method that can be seen as a systematic sampling of the space of possible values. We will thus refer to this method as DMCC (Discrete MCC) or MCC.

Although robust and easy to implement, this method presents some serious drawbacks, two of which are discussed here. First, systematic sampling is a rather slow algorithm for finding a maximum. This is especially true when the dimensionality of the problem grows and it can prove quite inefficient when the resolution of the sensor is high or the time span between the two images is long. However, the present use of this method for 24h ice drift retrievals from 1km resolution SAR images as performed e.g. at the Danish Technical University proves that the computer power available nowadays makes this particular drawback a nonissue, even for operational purposes. Second and more serious disadvantage, systematic sampling necessarily introduces a discrete sampling length (in our case, the length difference from one candidate pixel to its neighbors) which might prevent the accurate retrieval of the optimum point. In the case of ice drift, this sampling length directly translates into the well known “quantization effect”. This effect is most clearly seen where the displacements are small or draw a rotation pattern. Neighboring drift directions are “quantized” and show only approximate spatial continuity. This effect has so far prevented the MCC to be used for retrieving ice drift from pairs of images presenting too low a resolution-to-time-span ratio. For example, Ezraty *et al.* (2007a) produces 3 days ice drift from 12.5 km pixels images but the same authors chooses the AMSR-E (89GHz) images (6.25km pixels) to retrieve 2 days drift (Ezraty *et al.*, 2007b). By the same token, Haarpaintner (2006) applies the MCC to retrieve 2 days ice drift from Enhanced Resolution Quikscat/SeaWinds maps (2.225km grid).

By proposing a more continuous formalism to the optimization problem, we found that other methods than the MCC can readily be adopted which yield better results in terms of spatial smoothness of the displacement field yet with comparable computational needs. To put it briefly, it is illustrated that the quantization effect is not a curse of the low resolution satellite pixels but a drawback of using the systematic sampling MCC-like method (DMCC). As such, “sub pixel accuracy” can be achieved from the native resolution images, without over-sampling the pixels or using resolution enhancement techniques. This alternative method we refer to as Continuous MCC (CMCC).

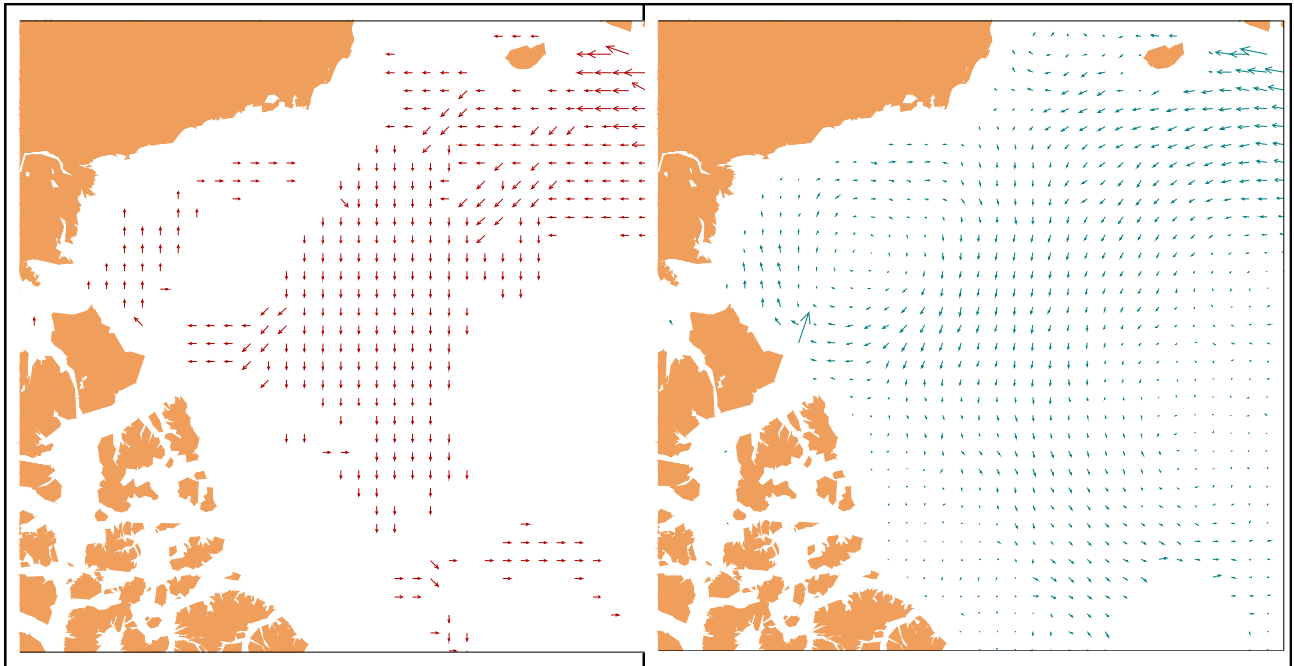


Figure 1: Example 48h ice drift products obtained from SSM/I images of the Beaufort sea and Canadian Basin using (left panel) the DMCC and (right panel) the continuous method investigated at met.no. Source images of 85GHz V-pol SSM/I ‘F15’ channel are dated from January 14th and 16th 2008. See text for more details.

Figure 1 proposes a visual comparison between (left panel) a 48h ice drift product retrieved via a DMCC implementation and (right panel) the ice drift product retrieved using the CMCC. In the left panel, white areas correspond to ice displacement vectors which were found with a length of less than half a pixel (except the blank area in the bottom right corner which stands for no-data because of the polar observation hole of the SSM/I, mostly visible in the right panel). The quantization effect is clearly seen in the left image whereas it has been removed in the right panel. At the basin scale, the retrieved field seems much smoother and more continuous with the new method than with the DMCC. For example, the rotation pattern of the Beaufort Gyre is more neatly drawn in the right hand side image. The erroneous looking arrow close to the shelf of Canada in the right panel would typically be removed by neighboring filtering applied at a later stage in the processing. Those filtering techniques are not investigated nor used by the authors at time of writing this report.

Still on Figure 1, the drift arrows are scaled by a factor of 2 thus not corresponding to true displacements over 48 hours. The spacing between each arrow is 62.5 km (5 x 12.5 km pixels) corresponding to the spatial resolution of the ice drift product. Daily averaged maps

of SSM/I 85 Ghz V-pol brightness temperature available through the OSI SAF were pre-processed via a Laplacian filter as proposed by Ezraty *et al.* 2007a. The remapping used is a polar stereographic grid with 12.5km spacing and true scale at 70 degrees north. It encompasses the Arctic Ocean, Greenland Sea, Baffin Bay and Davis Strait (see the domain displayed on top panels of Figure 5).

Each arrow is retrieved independently from its neighbors in the sense that no spatial smoothing term or regularization factor was used during the optimization, for both example products in Figure 1.

The continuous version of the MCC implements a simplex optimization method (Nelder and Mead, 1964)) to search for the maximum of the correlation function in the (x,y) space. When the method evaluates a vector which would be too long with respect to the maximum drift distance, the cross correlation is artificially reduced, thus forcing the optimization routine to stay in the desired radius. As is the case for the DMCC, blocks which are too close to land or to the ice edge are not processed. The CMCC does not allow retrieving more ice drift arrows but rather tends at improving the quality of the field by removing the quantization effect. A direct impact of this removal is the possibility to monitor ice drift over a shorter time period (e.g. 48h instead of 3 days) yet using the same sensors.

The processing chain implementing the CMCC at met.no is currently under development and testing. A first version of the production line and the first, Arctic region, 48h ice drift products from SSM/I, AMSR-E and possibly ASCAT should be available with a “demonstration” status in late 2008, via the Ocean and Sea Ice Satellite Application Facility (OSI SAF). The validation results presented in Section 2.2 are thus not representative of the final quality of the future product for which more extensive validation will be conducted.

2.1.2. In situ estimates of sea-ice drift

Numerous ice monitoring activities and deployment campaigns take place during the International Polar Year (March 2007 to March 2009). New ice drifters programs are launched and other are strengthened during this period. Although new instruments are designed to record more and more information on the state of the ice and its environment (e.g. sea temperature profiles for the Ice Tethered Profilers) the validation of ice drift products demands only limited input. Series of time and position records forming trajectories are enough to this exercise.

Historically, buoys from the International Arctic Buoy Program have been widely used for validating ice drift products. Although quite numerous, those buoys are mainly located in limited region of the Arctic Ocean (in the Multi Year Ice area north of the Canadian Islands and in the Central Arctic Ocean). Several investigators already reported that the positioning of those drifters (via the Argos system) could be erroneous and that the consistency of the trajectories should be carefully checked to make sure of the quality of those in-situ data. met.no receives and archives IABP buoys trajectories through the Global Telecommunication System (GTS). The Argos “quality flag” (from 1 to 3, 3 corresponding to a positioning uncertainty of less than 300m) was not found in these GTS data and further investigation will be conducted to be able to use that flag, if present. The time between each observation is typically of less than an hour but some trajectories presented some longer gaps.

The Ice-Tethered Profiler data are collected and made available by the Ice-Tethered Profiler Program based at the Woods Hole Oceanographic Institution (<http://www.whoi.edu/itp>). The level 1 raw data (“rawlocs.dat” files) are downloaded for all 13 active systems during winter 2007-2008. They contain GPS locations (typically every hour) and time for the record.

Filtering was applied to all the trajectories collected. A method similar to that of Hansen and Poulain (1995) was implemented to automatically detect bad positions. It works by computing the forward and backward velocities and screening them against a-priori knowledge. For this validation exercise, all 48 hours buoy trajectories presenting at least one “bad” point have been discarded.

The integrated, along-trajectory length was computed and all those buoys with a zero length over 48 hours were discarded. The discarded buoys were only those reporting their position through the Argos positioning system. It is believed that the absolute precision of this system does not allow for the 3 decimal digits latitude and longitude to stay exactly constant over 48h, thus pointing to a malfunction in the processing or reporting of the position information.

Finally, the in-situ 48 hours drift was computed as the vector between the position records closest to 12:00 UTC. The buoy was not used if those start and end points were not closer than 1 hour to 12:00 UTC. In-situ drift vectors are then remapped into the same polar stereographic grid than used for the ice drift product. Spatial collocation with the ice drift remote sensing product was achieved by computing a value of the product interpolated at the start location of the in-situ drift. A simple 2D interpolation between the 4 nearest neighbors was used.

2.2.Validation results

For a period covering 01/12/2007 to 29/02/2008 (start date of the products), 48h ice drift products obtained via the CMCC and MCC were collocated and compared to those from in-situ drifters. Comparison results for the SSM/I ‘F15’ 85Ghz V-pol processing are presented in Figure 2 where the CMCC (MCC) product is validated in the left (right) panel. Although the correlation factor and other statistics are similar in both cases, the validation graph in the left panel are clearly more satisfying than those on the right because the contour lines are more aligned around the 1-to-1 line. The shape of the contour lines on the bottom panel are a direct effect of the quantization effect, especially when a zero x or y drift component (on the Y axis) is retrieved via the MCC. Similar horizontal alignments can be observed around other “quantization” lengths (+/- 12.5km and +/- 25km). In the right hand side panel, the occurrence of intermediate drift component values is only due to the spatial collocation method we used (2D interpolation).

It should be noted that, unlike other investigators, validation results are not presented on North-South or East-West drift components but rather directly on the processing grid (see above). The transformation from a polar grid to a N-S and E-W one is quite a complex, non linear function whose effect varies with latitude and it was decided not to apply it before we can assess what level of deformation it implies to the comparison results. As such, our validation graphs (along the processing grid) cannot be compared with others (along N-S and E-W grid). This “along the grid” strategy is also the reason why the quantization of the MCC results appears in the validation, whereas a later transformation of the grid blurs it.

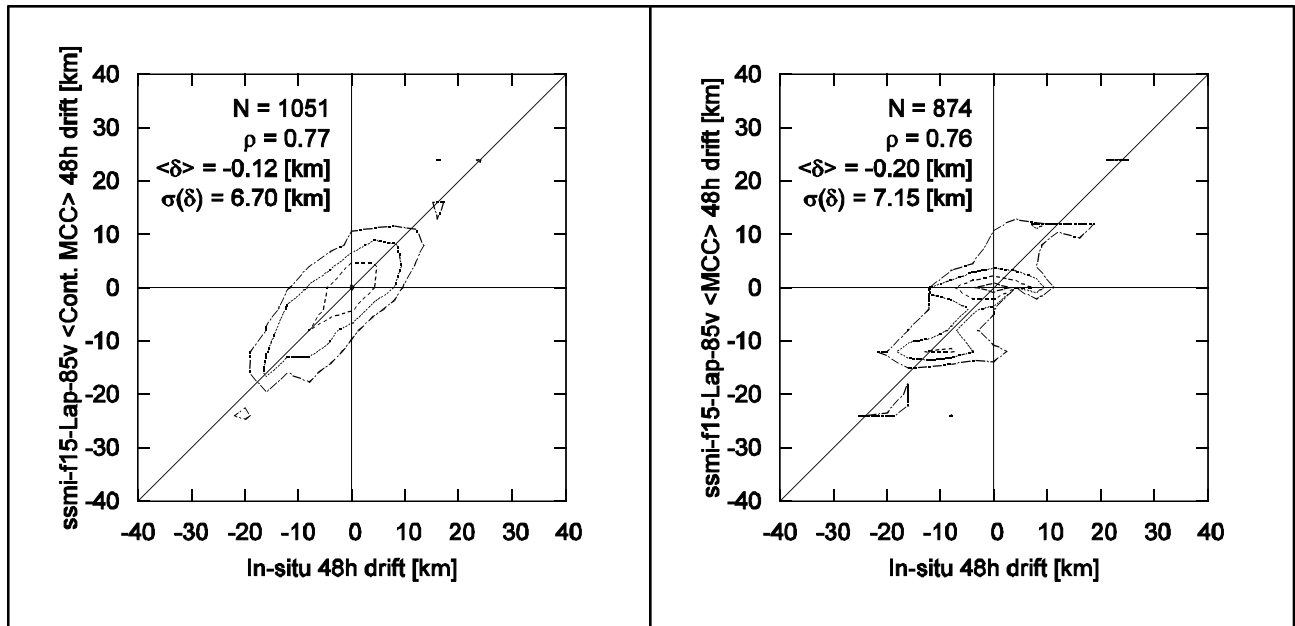


Figure 2: Validation result of the SSM/I 'F15' 85GHz-Vpol 48-hours ice drift product (Y-axis) obtained via the CMCC (left panel) and MCC (right panel) against in-situ 12:00 to 12:00 drifts (X-axis). The contour lines are delimiting regions of probabilities on a log-10 scale (outermost is $1e-8$, then every power of ten). Both x and y drift component enter in the comparison, km being counted along the x and y axis of the polar stereographic grid of the product. The number of samples (N) and the statistical correlation (ρ) are reported as well as the average and standard deviation of $\delta = \text{product-insitu}$.

Similar results are found when analysing the CMCC results applied on other instruments or polarization.

2.3. Conclusions and further research

An alternative ice drift processing method, the CMCC (Continuous Cross Correlation) is introduced which permits to search for the drift vectors in a continuous manner. Its main advantage is to remove the "quantization effect" which is seen as an artifact of the classic MCC (or Discrete MCC) while keeping the computation cost at an equivalent level. This directly translates in the possibility to reduce the time span of the ice drift processing to 48h drift vectors, also from 12.5km resolution sensors (SSM/I 85Ghz channels, AMSR-E 37GHz channels, ASCAT σ_0 , among others). The gained smoothness of the vector field is illustrated and confirmed by results of a validation experiment against in-situ drift estimates.

Further efforts are needed to give quantitative validation results over a longer time period. In the context of this short validation period, we observed a systematic dependency of the comparison quality with the sensing time in the pair of images and it should be assessed how the 48h ice drift vectors are sensible to that parameter (see also next section).

3. MERGING ICE DRIFT DATASETS FROM DIFFERENT SOURCES

In this section, we present and illustrate results from our investigation concerning the merging of ice drift product when estimated from different sources. First we review the motivation that justify merging and briefly present the methods currently applied by other authors. Then, we show that those methods cannot be implemented as is to our new “continuous” ice drift dataset but that we can access some estimate of the uncertainty of each vector we want to merge. This uncertainty measure should ease the computation of a best vector from the various sources. Finally, we give example of situations where the gain in accuracy allowed by the CMCC is such that it discourages the merging of datasets when they are not approximately collocated in the time period they cover.

3.1. Justification for the merging and currently implemented methods

Nowadays, when dealing with Arctic ice drift processing from low resolving satellites, there is more data available than we need. Platforms on polar orbits, combined with the large swaths of the instruments considered provide several times a complete coverage of the Arctic regions every day. It is thus largely feasible to get daily coverage of ice drift products from, say, SSM/I (3 platforms currently flying), SSM/IS, AMSR-E, ASCAT, etc... Moreover, some of those instruments operate in several wavelengths and in several polarizations which allow us to count on 5 or more independent ice drift datasets on a daily basis (e.g. SSM/I 85GHz-Vpol, SSM/I 85GHz-Hpol, AMSR-E 37GHz-Vpol, AMSR-E 37GHz-Hpol and ASCAT C Band σ_0). This abundance of independent data is the starting point to the merging of the ice drift datasets, process which aims at 1) a better coverage of valid vectors (in region where 1 or more of the processing fails to retrieve a valid vector) and 2) a better confidence in the “merged” vector than in the one of the individual products.

Merging products from two different platforms is unlike merging those from the same instrument. It seems indeed easier to merge for example EOS-Aqua’s AMSR-E 37GHz-Vpol with EOS-Aqua AMSR-E 37GHz-Hpol than with SSM/I ‘F15’ 85GHz-Vpol. The main reason is the difference in the acquisition time of the pair of images. It is a-priori desirable to perform both type of merging (intra- and inter-platforms) but our investigations confirm that the inter-platform merging should be performed with greater care.

Intra-platform merging of ice drift products has often been performed by ice drift investigators. This type of merging is thought more straightforward as it usually involves two independent sources (2 polarizations). Haarpaintner (2006), for example, computes the merged ice drift vector as the average of the displacements obtained from processing pairs of horizontally and vertically polarized images from the QuikSCAT/SeaWinds instrument (Haarpaintner (2006), Section III.C). It is to be noted that when the individual ice drift products are retrieved with the discrete MCC, this averaging might introduce some level of angular smoothness in the merged dataset, by reducing the quantization effect. This averaging method can readily be (and has already been) applied to each pair of SSM/I ‘F15’ 85Ghz products (Vpol & H-pol) and EOS-Aqua AMSR-E 37Ghz (V-pol & H-pol). Although valid, this method might be somewhat simplistic as the full information content of the individual vectors is not taken into account (see Section 3.2.1).

Inter-platform merging can be achieved with various levels of complexity. The “raw composite” (term employed by Ezraty et al. 2008) is the simplistic filling of non valid drift locations in the product we trust most by valid drift vectors from the other sources. This first approach is rather

straightforward and allow filling up the product grid with valid vectors (Ezraty et al. 2008, Figure 1). A more advanced algorithm is presented by Ezraty et al. 2008 which merges ice drift products from SSM/I 85GHz V-pol, SSM/I 85GHz H-pol and Quikscat. A hierarchy of 14 cases is designed so that the best vector is chosen taking into account the a-priori confidence one has in each product, the level of agreement between the retrieved arrows at one location and, finally, the agreement with the neighboring estimates. A selection process, this algorithm never performs averaging between vectors and ice drift estimates in the merged product can always be traced back to one of the source datasets. This advance merging technique however presents some drawbacks for its application to other processing chain. Firstly, it relies on the a-priori confidence one has on each product. This confidence in the individual retrievals might however vary in space and time and it seems somewhat awkward to elect a favorite data source for the whole Arctic region and for a whole winter. Second, it seems difficult to extend the method to more than three data sources. The number of possible cases would indeed rapidly increase to form a much more complex decision tree. Even applying the algorithm as-is on 3 data sources (intra platform merged SSM/I 85GHz-HV, intra platform merged SSM/I 37GHz-HV and ASCAT σ_0) is not a viable alternative as the intra-platform merged product seldom agrees due to the averaging between vectors. It is even more so if the CMCC is used.

In the next section, we will show how some level of information of the uncertainty in the drift estimate lies in the shape of the correlation function around its maximum and provide hints of how this uncertainty information could be used to merge ice drift products.

3.2. Assessing the uncertainty in ice drift estimates acquired from pairs of images.

3.2.1. Qualitative assessment

Motion retrieval from pairs of images works by identifying patterns common to both images. It is thus of common understanding that the sharper the intensity variations in the images are, the more accurate the motion estimate will be. Ice drift vectors retrieved between images presenting limited variation in their intensity field (weak intensity patterns) should be less certain than between images with clear intensity changes. By the same token, ice drift, when tracked manually by operators in the national ice services, is retrieved between clear patterns that stand out from the remaining of the image.

Figure 3 proposes a visual representation of the contour lines of the correlation function $\rho(x,y)$ for two data sources, namely AMSR-E 37GHz – Vpol and Hpol. In that example, pertaining to a 48h drift starting on January, 1st 2008 at 12.00 and retrieved using the continuous MCC, both ice drift estimates agree and were computed on a section of the images presenting definite intensity patterns (for both polarization, only the horizontal one is displayed on the right panel of Figure 3). The peak of $\rho(x,y)$ is accordingly concentrated around the best value and we can qualitatively present these two estimates as “certain”. It is to be noted that the classic MCC would return a 0-length vector at this location. Although this result is in the $\rho > 0.9$ ellipse, it is bound to be more uncertain than the one we can retrieve with the continuous MCC, and is a direct consequence of the quantization effect.

Figure 4 displays a different situation arising from analyzing the SSM/I ‘F15’ 85GHz V and H pol products. Unlike on Figure 3, both polarizations do not agree in terms of the ice drift vector, with a relative angle of around 40 degrees. However, the vertical channel (solid line) yields a sharper peak for its correlation function than the horizontal one (dotted line). This also corresponds to weaker patterns in the images itself (visual assessment, not shown).

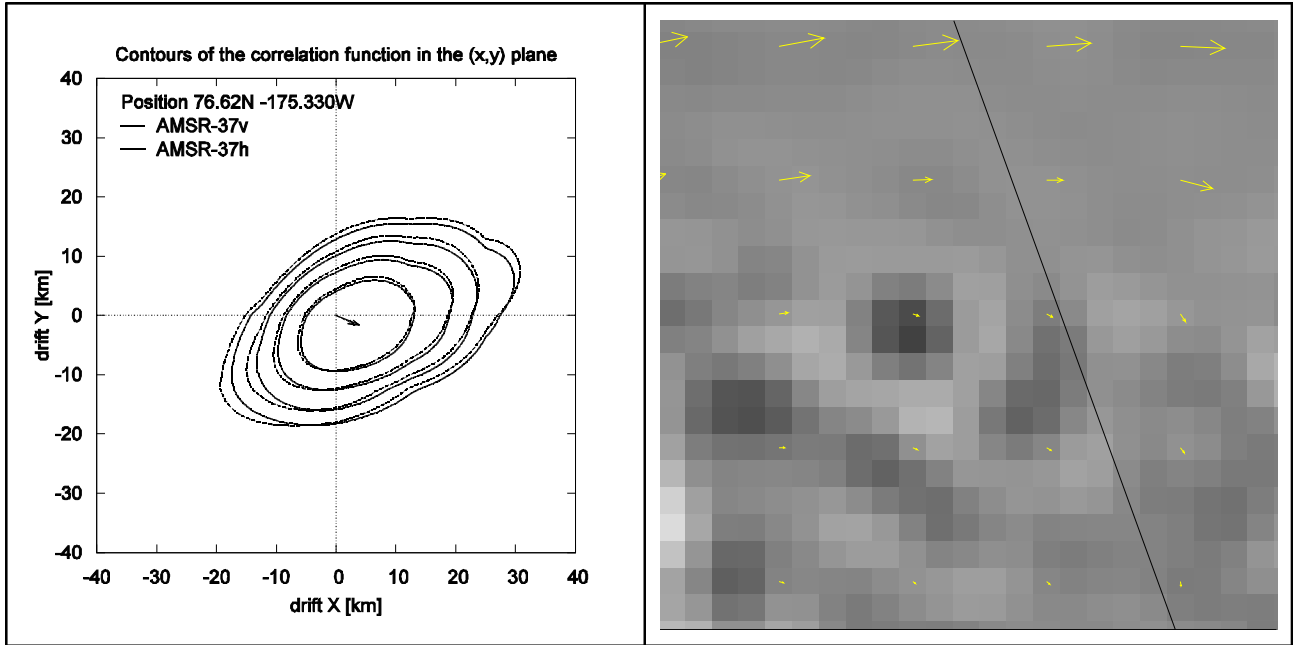


Figure 3:

Left panel: Example contour lines for the correlation functions obtained by processing two polarizations of the AMSR-E 37GHz signal. The maximum correlation is at the tip of the drift arrow and defines the retrieved ice drift. Contour lines for $\rho=0.9, 0.8, 0.7$ and 0.6 are shown.

Right panel: Corresponding (laplacian of) AMSR-E 37GHz-Hpol image showing several surrounding drift vectors. The drift vector corresponding to the left panel is near the centre of the image, inside the dark pattern.

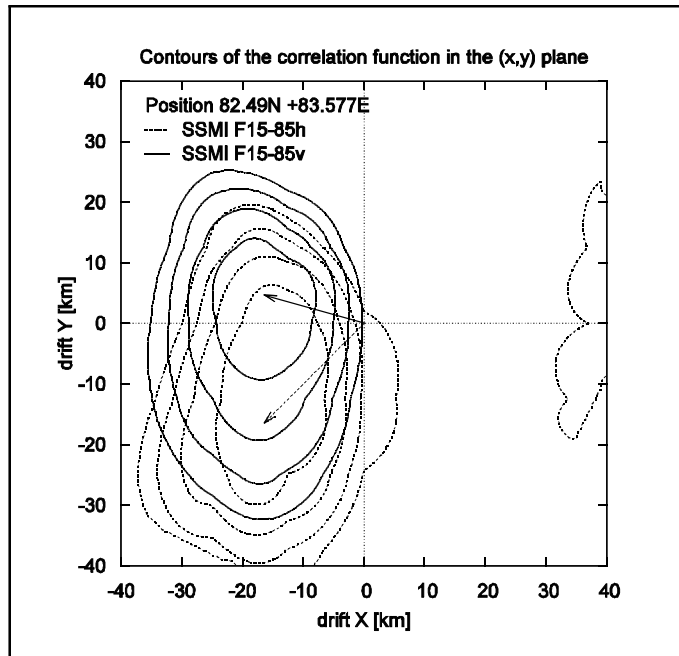


Figure 4: Same as previous except that the data sources are SSMI 'F15' 85Ghz V and H polarizations. The geographical position of the drift estimate is also different. In that example, both polarizations do not lead to the same drift estimate also using the 85V channel (solid line) yields a more certain vector, in terms of sharpness of the correlation peak.

The maximum correlation for the vertical channel is even in the $\rho > 0.9$ region of the horizontal channel.

Figure 4 typically displays a situation where merging vectors by an evenly weighted average of two polarizations (Section 3.1) is not optimal. It also gives insight on how the merging of datasets could benefit from the quantitative knowledge of the uncertainties on each source vectors. This uncertainty quantities at hand, weighted averages of the Probability Distribution Functions give the most robust and accurate mean for computing merged products, that is the drift vector as well as its final uncertainty.

Our investigations also illustrated that the shape of correlation function varies not only between polarization channels of a wavelength, but also, and as is expected, between wavelengths (85Ghz vs 37Ghz or C-Band σ_0). If quantitatively assessed, this should allow to access geographically and temporally varying confidence level in our retrieved source products, as inputs to the merging process. Finally, it should be mentioned that the contours of the correlation function behaved as expected when the ice drift was processed from artificially smoothed images, the peak broadening until being flat for flat images intensities.

3.2.2. Quantitative assessment

The quantitative assessment of uncertainties aims at providing the covariance matrix of the uncertainties for each drift pixel, that is the standard deviation of the uncertainty in the x (y) displacement σ_x (σ_y) and the correlation between both uncertainties ρ_{xy} . Under a Gaussian hypothesis, those quantities, along with the mean vector (x,y), completely characterize the PDF on the retrieved quantity. This *a-posteriori* PDF is needed for assimilation applications (observation error covariance matrix) as well as for merging datasets.

The quantitative derivation of those uncertainties could however not be obtained during this project and will require more investigations. Some points however can be readily made:

- The sharpness of the correlation peak (in the x,y space) is directly linked to (some function of) its second derivatives, entering the Hessian matrix. The exact relation should be investigated. Second derivatives of the correlation function can be computed by finite differences.
- The formalism underpinning the Inverse Problem Theory (and especially of the Bayesian case) (Tarantola 2005) is mainly built around minimizing the sum of the squared differences (between the images) and not around maximizing the correlations. It might prove difficult to find equivalences between the two methods.
- The discrete MCC applied on low resolving satellite images does not allow this characterization because the correlation function is poorly sampled around the maximum and thus looks noisy. It might be less of an issue for high resolution images.

Uncertainty on the retrieved quantity is a goal per se that should be pursued for all remote sensing datasets. In this section, we showed evidence that the shape of the correlation function in the x,y space could be qualitatively understood as an uncertainty information. A quantitative estimate could be used both for the assimilation of this ice drift product in ocean/ice coupled models and to allow a better merging of the datasets, at least for the intra-platform merging.

3.3.Limits to merging ice drift datasets from different sensors.

3.3.1.Accounting for the exact time span of the ice drift products

Intra-platform merging of datasets can safely be implemented as the images have exactly the same time stamp, thus yielding ice drift vectors for the same period [T0, T1]. In this section, we illustrate that inter-platform merging should maybe be handled with more care, especially when the acquisition times of the swath data differ to much or when certain extreme weather patterns drive the ice displacements.

In the satellite ice drift community, two approaches are frequently opposed. The first one computes the ice drift between pairs of composite maps (usually an average of the swath during one day) which covers entire basins or ocean (e.g. Ezraty et al. 2007a, Haarpaintner 2006). Those daily maps have been used by many investigators (also in this study) for the processing of ice drift from low resolving satellite images. It is commonly accepted that the vectors are then representative of an average drift over the period, or at least are not usually associated to specific start and end time others than the central time for the composite images¹. Ice drift from high resolution data, however, has only been computed (to our knowledge) between pairs of swaths, thus keeping an exact information of the start and end time for their vectors. The reason for this choice is obviously the blurring that would be induced by averaging drifting ice pixel intensities from different 1km resolution swaths, the scale of the ice motion between two subsequent swaths being of the order of the pixel resolution. The same motion is expected to blur and degrade the enhanced resolution ice datasets, e.g. the one from QuikScat/Seawinds dataset (Haarpaintner, 2006).

Avoiding the definition of exact time stamps, several investigators have merged low resolution products processed from daily maps, acquired by different instruments on different platforms (see references given in Section 3.1), to achieve a better coverage. Maybe because of the somewhat shorter time range (48h) we have been computing the ice drift over or maybe because of the enhanced quality provided by the use of the CMCC, our investigations lead us to be more cautious when merging those datasets.

A case study is presented in the next section that illustrates a typical situation where the inter-platform merging is difficult to achieve.

¹ Although Haarpaintner (2006) has access to an average start and end time for the vectors, he also mentions (Section V) not using them. He thus associates an identical start and end date for all the ice displacement estimates.

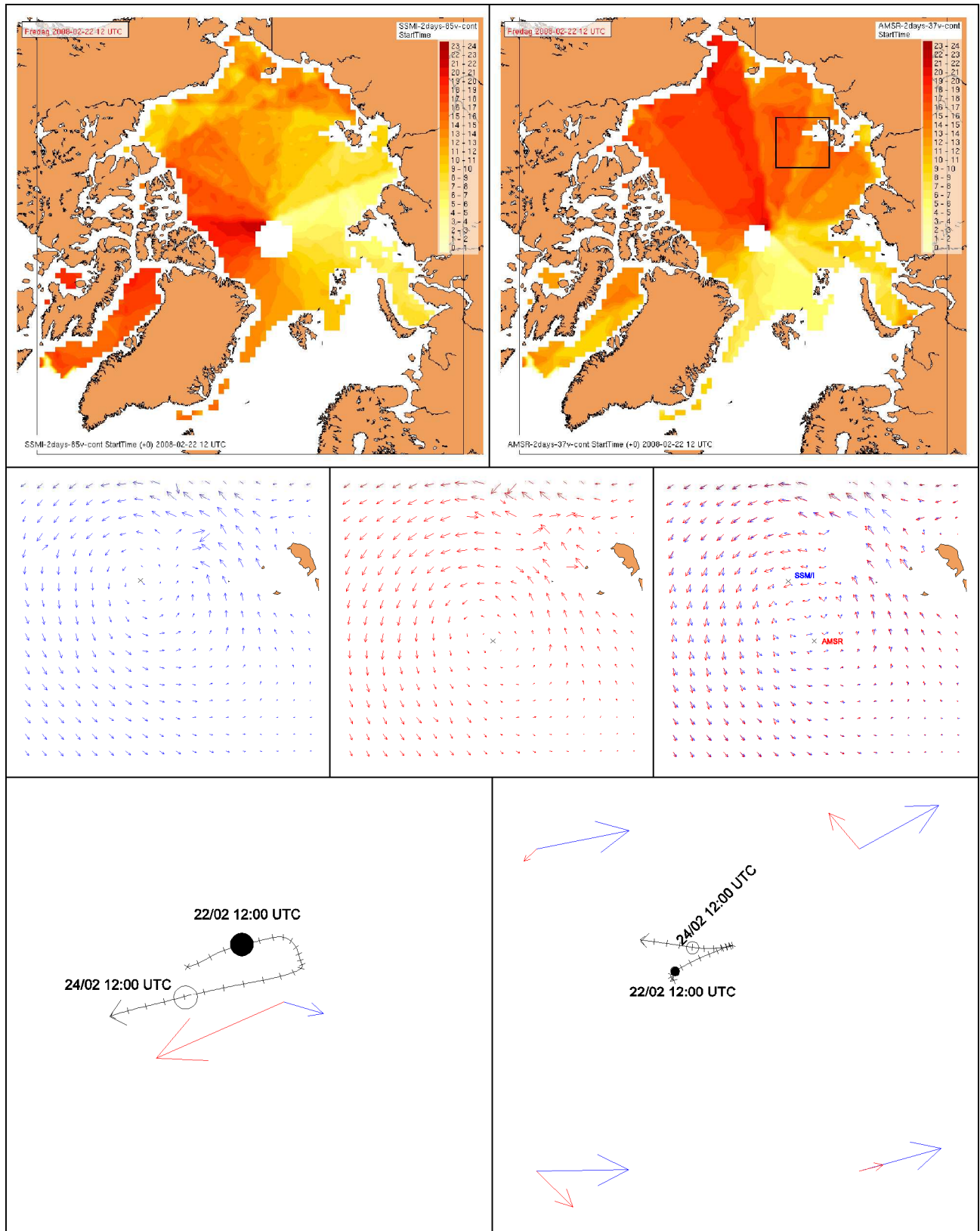


Figure 5: A rapidly moving low pressure system passes over the ice shelf north of Novosibirskiye Ostrova (Russia) during the February 22nd to 24th (2008) period. Refer to the text for figure description.

3.3.2. Case study: 48h ice drift generated by a low pressure system traveling over the ice shelf north of Siberia. On the importance of the exact time period.

Figure 5 presents the analysis of a case study where the 48h ice drift acquired from averaged daily maps of SSM/I 85Ghz-Vpol and from AMSR-E 37GHz-Vpol do not agree. The daily maps were built from available swath data for February 22nd 2008 (from 00UTC to 24UTC) and February 24th 2008 (idem). Although an exact time stamp cannot be given to each pixel, an “average” time, defined as the average of the time stamps of the individual swaths which contributed to the daily map intensity for each pixel, can be computed and is displayed at the Arctic scale for the SSM/I daily map (top-left panel) and the AMSR-E (top-right panel). Shades of yellow to dark red are scaled with the average hour in the day. A pale yellow color thus corresponds to locations where the intensity field has been mainly sensed early in the day (e.g. 9AM) and red areas to late sensing times (e.g. 6PM). Only the average time of the first image of the pair is displayed in Figure 5, thus corresponding to the start time of the retrieved ice drift. Thanks to the characteristics of the orbits of both satellite platforms, the average end time is for all practical purposes similar to the start times, at least for latitudes corresponding to the Arctic Ocean.

During the considered period, a low pressure system rapidly passes (from east to west) over the ice shelf, north of Novosibirskiye Ostrova (Russia) and induces a counter-clockwise circular pattern (radius of approximately 300km) in both 48h ice drift products. Those are displayed individually on the middle line left (SSM/I) and centre (AMSR) panels. As on Figure 1, yet unfiltered outliers appear in both fields, especially in the vicinity of the island. Those were manually removed in the right panel (middle line) where both products are superimposed. The centre points for the rotation patterns (black cross) are also reported on the images (visual estimation). They are fairly apart and the distance between them is estimated to 200km. As a matter of fact, ice drift estimates from the two sensors do not agree when compared pixel-by-pixel. Careless merging of those two vector fields would undoubtedly lead to a quality loss and a weakening of the rotation pattern in the movement.

By comparing the average time (top panel) for the region of the Arctic Ocean under study it can be noted that, although both are 48h drifts starting during February 22nd, the vector field estimated from SSM/I images comes earlier (start time around 10 AM) than the one from AMSR-E images (start time around 5 PM). This 7 hours time lag in the drift period is visually consistent with the east to west displacement of the rotation pattern, induced by the passing low pressure.

Some conclusions can readily be drawn. It is illustrated in this section that, although retrieved from low resolution satellite images, the 48h datasets we are able to retrieve using the continuous MCC are sensitive to the actual start and end times at which the swath data used to compute the daily maps were taken. This implies that 1) users should be given the necessary information to accurately locate in time each ice drift vector, 2) the validation against buoys should ideally be conducted taking this exact period into account (unlike in Section 1 of this report) and 3) that optimal merging algorithms should take into account the time difference between the vectors. To our knowledge, points 1 and 2 are only applied for high resolution datasets which make use of swath data and point 3 is not put into practise in the merging of low resolution products.

The bottom panel of Figure 5 is meant at illustrating point 2 above. The (approximate) center of both rotation patterns were drifted by the output ice velocity fields (ice.u and ice.v) of the coupled ocean sea-ice model run operationally at met.no for forecasting the state of North Atlantic and Arctic regions. The model (MI-POM / MI-IM) has a spatial resolution of 20km. In operation, it is forced by the ECMWF analysis and 10-days forecast. The trajectory on the left (right) panel corresponds to the motion of the center point of the SSM/I (AMSR-E)

circular pattern (see above). Along the trajectory, the black-filled disk symbols correspond to a time stamp of 12:00 on February, 22nd 2008 and the empty disk symbols to the same hour on February 24th. Those times are thus the central one for both pairs of daily SSM/I (AMSR-E) brightness temperatures maps. Ticks along the trajectory are every 3 hours. With a visual analysis of the left panel, one can verify that in this region, a drifting ice volume starting around 9AM (and lasting for 48h) is a limited, westerly ice drift. This corresponds somewhat to the small SSM/I (blue) arrow which is at the closest grid point in the product. Conversely, a 48h drift starting around 5PM is a longer, northerly drift much similar to the AMSR-E product (red). The same exercise can be repeated along the trajectory displayed in the right panel. Finally, in both panels, one can see the disagreement between each individual ice drift product and the displacement the model proposes from 12:00 to 12:00.

When taking into account the start and end time, visual agreement between the model ice drift and the products we were able to produce is encouraging. In the remaining mismatch lies the benefit such a coupled ocean and ice model could gain from assimilating these remote sensing products.

3.4. Conclusion on merging of ice drift datasets

In this section, we have made a clear distinction between intra-platform merging (for ice drift products retrieved from pairs of images from a unique instrument or from instruments on the same platform) and inter-platform merging (when the ice drift is processed from images acquired by different instruments).

In the case of intra-platform merging (for example SSM/I 'F15' 85GH-z V-pol with the corresponding H-pol), we have qualitatively assessed that the sharpness of the intensity patterns in the source images translates in a sharpness of the correlation peak around its maximum in the (x,y) space. The broadness of this peak can be interpreted as a measure of the uncertainty on each retrieved ice drift vector. We proposed that merging should always take into account this uncertainty. We gave hints and reference to the Inverse Problem Theory and Bayesian formalism that could provide suitable strategies. The challenge, unresolved in this report, lies in the to-be-found equivalence between maximizing a correlation and minimizing squared differences.

For inter-platform merging (for example SSM/I 'F15' GHz V-pol and AMSR-E 37Ghz V-pol), we reported on a case study where the low-resolution ice drift products processed from daily maps presented a clear signature with respect to an average start and end time for pixels in the daily composite images. The regional spatial patterns of the ice-drift fields could be explained by a coupled ocean and ice model provided the actual drift period was considered. We agree that the signature of a low pressure system is a somewhat extreme example, even more so with a 7 hours time lag between the average start times and in regions of somewhat thin First Year Ice. It remains however that 1) to our knowledge, currently applied merging techniques do not take this effect into account and that 2) more investigations are needed to provide more accurate low resolution merged datasets. A statistical comparison between the inter-sensor differences and the lag between the start times would be a sensible start in order to quantify this effect.

4. ACKNOWLEDGEMENTS

This research effort could not have been possible without the support of the Research and Development Department of the Norwegian Meteorological Institute. The authors thank the various ice drift investigators which indirectly contributed to this research through insightful and challenging discussions.

5. REFERENCES

- Hansen, D. and Poulain, P.-M. Quality control and interpolations of WOCE-TOGA drifter data (1995), *J. Atmos. and Ocean. Tech.*, vol. 13.
- Ezraty, R., Girard-Ardhuin, F. and Piollé, J.-F. Sea-ice drift in the central Arctic estimated from SeaWinds/QuikSCAT backscatter maps - User's manual, CERSAT, IFREMER, France (v2.2, Feb. 2007)
- Ezraty, R., Girard-Ardhuin, F. and Piollé, J.-F. Sea-ice drift in the central Arctic combining QuikSCAT and SSM/I sea ice drift data - User's manual, CERSAT, IFREMER, France (v3.0, April 2008)
- Ezraty, R., Girard-Ardhuin, F. and Croizé-Fillon, D. Sea-ice drift in the central Arctic using the 89GHz brightness temperatures of the Advanced Microwave Scanning Radiometer – User's manual, CERSAT, IFREMER, France (v2.0, Feb. 2007)
- Haarpaintner, J. (2006), Arctic-wide operational sea ice drift from enhanced-resolution QuikScat/SeaWinds scatterometry and its validation, *IEEE Trans. Geosci. Remote Sens.*, vol. 44, no.1, pp.102-107, Jan. 2006.
- Maslanik, J., T. Agnew, M. Drinkwater, W. Emery, C. Fowler, R. Kwok and A. Liu (1998), Summary of ice-motion mapping using passive microwave data, *National Snow and Ice Data Center (NSIDC)*, Special Publication 8.
- Nelder, J.A., and Mead, R. (1964). A simplex method for function minimization, *The Computer Journal*, 7, 308-313.
- Tarantola, A. (2005), Inverse problem theory and methods for model parameter estimation, *SIAM, Philadelphia*.